Contents lists available at ScienceDirect

Optical Materials

Spectroscopic properties of UV active medium Ce^{3+}:LiSr$_{0.8}$Ca$_{0.2}$AlF$_6$

A.S. Nizamutdinov *, A.A. Shavelev, M.A. Marisov, V.V. Semashko

Kazan Federal University, Kremlevskaja Str., 18, Kazan 420008, Russian Federation

A B S T R A C T

The aim of this work is phase composition and near UV spectroscopic studies of UV active media in fluoride crystals with colquiriite structure, such as Ce^{3+}:LiSr$_{0.8}$Ca$_{0.2}$AlF$_6$. Colquiriite structure mixed crystals show higher segregation coefficient of Ce^{3+} activator ions than common LiCaAlF$_6$ hosts. An important result is based on the fact that this enhancement was achieved for two types of Ce^{3+} centers in a multisite Ce:LiSr$_{0.8}$Ca$_{0.2}$AlF$_6$ system. Thus, it provides a higher gain coefficient for the 5d–4f transitions of Ce^{3+} ions and it spans a wider continuous wavelength tuning range between 280 and 320 nm for tunable Ce: LiSr$_{0.8}$Ca$_{0.2}$AlF$_6$ laser systems.

1. Introduction

Since the discovery of direct UV laser oscillation from Ce^{3+} doped LiCaAlF$_6$ (LICAF) crystals [1], the gain medium has been investigated for various applications [2–4]. Significant vibrational broadening of the 5d–4f transitions of Ce^{3+} ions for extended laser tunability was used in LIDAR systems for remote atmospheric control [5]. Higher cross-sections of dipole interconfigurational transitions provide a lower threshold for laser oscillation. Coupled to the appropriate pumping source this system exhibited tunability from 281 to 316 nm [5], with more than 60 mJ output energy from the oscillator [6] at 290 nm and high repetition rate, up to 20 kHz [7] with fast and robust operation. Up to now, microchip UV lasers were investigated [8] and lasing was achieved with 24% slope efficiency from a 2.2 mm long Ce,Na:LICAF crystal with a Ce ion dopant concentration of 3.5% in the melt, and 2 μJ pumping energy at 266 nm from a microchip Nd:YVO$_4$ laser device. Interesting results have been achieved too in the field of short pulses. UV laser pulses of 22 ps at FWHM were obtained [9] by using synchronous pumping with 70 ps laser pulses. Also, laser pulse trains have been achieved with 800 ps at FWHM for a single pulse, from a low Q cavity [10]. Generation of short laser pulses is not a trivial task as mode-locking or Q-switching techniques must be employed and control of optical cavity's Q-factor was obtained by modulating optical cavity transients [11,12].

Any further progress of Ce-doped colquiriite lasers is associated with improvement spectroscopic and photochemical properties of the crystals and increment of dopant's concentration. It is widely accepted that Ce^{3+} activators in Ce:LICAF matrixes are able to substitute sites occupied by Ca^{2+}, which has an ionic radius similar to that of Ce^{3+} (1 Å and 1.03 Å, respectively) [2]. However, it is difficult to increase the Ce^{3+} ion concentration in Ce:LICAF crystals because the valences of Ce^{3+} and Ca^{2+} ions are different. An increment of dopant's concentration has the consequence of enhancing crystal lattice defect generation, as the crystal strangles to preserve its electric neutrality. Consequently, the segregation coefficient of Ce^{3+} ions in Ce:LICAF crystals is quite small [13,14]. Moreover, Ce^{3+} ions doping produces "seed centers" for color center generation. It is known that by varying the chemical structure of the compound, by adding a set of crystal lattice cations in the matrix, one can improve the optical quality of the crystals by increasing the isomorphic capacity of the solid solution [15].

By growing mixed LiSr$_{1-x}$Ca$_x$AlF$_6$ crystals with varying x, is possible to optimize the chemical content for improving laser properties. In earlier works [16,17], a series of LiSr$_{1-x}$Ca$_x$AlF$_6$ crystals activated with Ce^{3+} ions exhibited a higher absorption coefficient for Ce^{3+} ions, which could be an advantage for activator ions concentration optimization with subsequent laser action [17,18]. Furthermore, it should be noted that multicenter Ce^{3+} segregation in colquiriite crystals plays a significant role for laser action while the distribution of Ce^{3+} ions concentration among different types of impurity sites in mixed crystals is unclear. Indeed, the ionic distribution depends not only on the Ca/Sr ratio but on the crystal growth conditions also and crystals grown by the Czochralski method have a lower segregation coefficient of Ce^{3+} ions in comparison to the Bridgman growth technique.

* Corresponding author.
E-mail address: anizamutdinov@mail.ru (A.S. Nizamutdinov).

In earlier works different models of Ce^{3+} ion impurity sites in LICAF host lattices were investigated via comprehensive site-selective time-resolved fluorescence and EPR spectroscopies [19,20].

In this work, both the spectral and kinetic characteristics of Ce^{3+}:$LiSr_{0.8}Ca_{0.2}AlF_6$ colquiriite mixed crystals grown by Bridgman–Stockbarger method are presented. The article is organized as follows: first, the methodology, growth of crystals and preparation is presented. Next, the optical and chemical properties of single and mixed crystals are compared via absorbtion, X-ray, excitation and time decay spectroscopies and potential applications for UV solid state lasers are discussed.

2. Experimental

2.1. Materials and methods

Generally, high chemical purity of starting materials is a key factor to grow fluoride crystals for laser applications. Removing traces of oxygen and hydroxyl groups is the most critical. Furthermore, the performance of the solid-state laser crystal media is affected by their optical quality and the number of crystal defects, which in turn, are influenced by the crystal growth conditions and the final polishing. In particular, one of the main problems arising from the operation of materials under intense UV radiation is the degradation of their optical properties colquiriite crystals demonstrate high stability toward UV irradiation, while Ce:LICAF has the highest stability of laser efficiency [21].

$LiCaAlF_6$ and $LiSr_{0.8}Ca_{0.2}AlF_6$ crystals doped with 1 at.% of Ce^{3+} ions in the melt were grown by Bridgman–Stockbarger in closed graphite crucibles. This growing technique maintains the chemical composition of the melt and allows growing crystal samples with different activating ions, even for low segregation coefficients of impurities, in contrast to Czochralski technique.

The melting point of the crystals is 810 °C [13]. These systems are multicomponent, and, as indicated above, they are characterized by a low segregation coefficient of the Ce^{3+} ions. Therefore, it is critical to arrange a sufficient temperature gradient in the crystallization zone during the growing process [14]. The temperature gradient is 120 K/cm and it is provided by the appropriate design of geometry of the heater, the heat shields and the crucible.

Because the components contain aluminum fluoride as a starting material, which has high saturated vapor pressure and does not exist in a liquid phase, overheating of the melt will lead to a depletion of this component. Also, temperature is set higher than the melting point (20 °C) to ensure melting and homogeneous mixing of the substances.

The initial concentration of CeF_3 was 1 at.%. Oriented cylindrical crystals 10 mm wide and 80 (Ce:LICAF) and 20 mm (Ce:LISCAF) long were grown under the above conditions. A series of samples for optical spectroscopy were prepared from the synthesized crystals. For Ce:LICAF crystal polished plane-parallel windows were made along the boule and for the Ce:LISCAF crystal plane-parallel plates with polished windows were prepared. The optical c-axis was in the plane of the polished windows.

2.2. X-ray diffractometry

The phase composition of crystallized material was investigated by an X-ray diffractometer (Shimadzu powder diffractometer XRD-7000S) at room temperature and fine powder samples were prepared from the crystals. And the reflection distributions are shown in Fig. 1.

The diffraction pattern for the Ce^{3+}:LISCAF samples corresponds to a colquiriite structure and reflections are lying between the LICAF and LISAF ones [22–24], as is expected.

The diffraction lattice constant was concentration ratio dependent for both mixed and unmixed samples (Fig. 2).

The lattice constants for the Ce^{3+}:LISCAF crystal are placed somewhere along the straight lines between the LICAF and LISAF ones. Therefore, the crystal is monocrystalline and it has only one phase according to Vegard's rule.

3. Optical spectroscopy

3.1. Absorption spectra

Spectroscopic investigations of Ce:LISCAF crystals grown by Czochralski method with different Ca/Sr ratio concentrations, were performed earlier [16,17] and a red shift of maximum of single absorption band at 270 nm of Ce^{3+} for pi-polarization with increasing Ca^{2+} concentration was detected owing to the lessening of the lattice constant. A red shift was not observed for a sigma-polarization component [17]. As the Ca^{2+} concentration varies, there is an extremum of the absorption coefficient at 266 nm for a 0.25 ratio of the Ca/Sr content having an absorption coefficient of 7 cm^{-1} for 0.5 at.% of Ce^{3+} ion concentration in the melt.

In Fig. 3 the absorption bands for the lowest 4f–5d transition of Ce^{3+} ions in LICAF and LISCAF crystals grown in this work are shown. There is a small red shift in the absorption spectrum with increasing Ca^{2+} concentration, in agreement with [17]. However, this is a superposition of a number of spectral bands corresponding to different nonequivalent impurity Ce^{3+} ion centers [20].

It is worth noting that the absorption coefficient of the mixed Ce:LISCAF crystal grown in this work is five times greater than the absorption coefficient of the Ce:LICAF crystal (Fig. 3).

3.2. Luminescence and excitation spectra

Excitation and luminescence spectra for a number of excitation wavelengths were obtained. Excitation spectra are nonpolarized and were recorded from bulky samples in a Perkin–Elmer Lambda LS55 spectrofluorimeter. Both luminescence and time decay spectra were recorded from the same samples with a scanning monochromator MDR-23, with a 1200 line/mm grating, and a fast photomultiplier tube (FEU-79) coupled to Tektronix DPO 7354 oscilloscope with 3.5 GHz bandwidth. The crystals were excited in the spectral range from 240 to 290 nm by the third harmonic generation of a tunable Ti:Sapphire laser, (10 ns at FWHM and 10 Hz repetition rate).

In Fig. 4 the luminescence spectra at room and liquid nitrogen temperatures are presented. The room temperature spectra of Ce:LICAF crystal depend strongly from the excitation wavelength, compared to the spectrum of Ce:LISCAF. As it was shown in [20], three types of Ce^{3+}-impurity centers contribute to the luminescence spectra. First, Ca^{2+} ionic sites with nonlocal charge compensation ((a) bands at 281 and 300 nm). Second, Ca^{2+} ionic sites with a Li^+ vacancy in the nearest cell ((b) bands at 287 and 307 nm) and third Al^{3+} ionic sites ((c) center bands at 310 and 332 nm). These luminescence are marked with color lines similar to [20].

The Ce:LISCAF luminescence spectra appear to be the simplest ones. A small red shift from mixed Ce:LISCAF crystal to Ce:LICAF is observed due to change of lattice constants for different Ca/Sr concentration ratios, in agreement with [17] and absorption spectra. Excitation near the longer and shorter wavelength shoulders of the absorption bands (275, 255 and 245 nm) in Ce:LICAF register the spectral signature of a (c)-type center at 310 nm and 330 nm. This is not observed with an excitation wavelength at 266 nm,
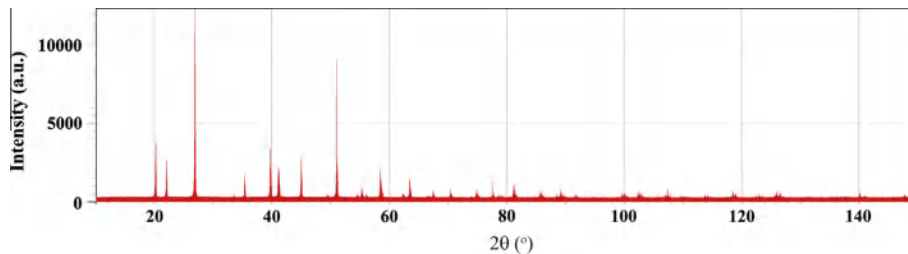
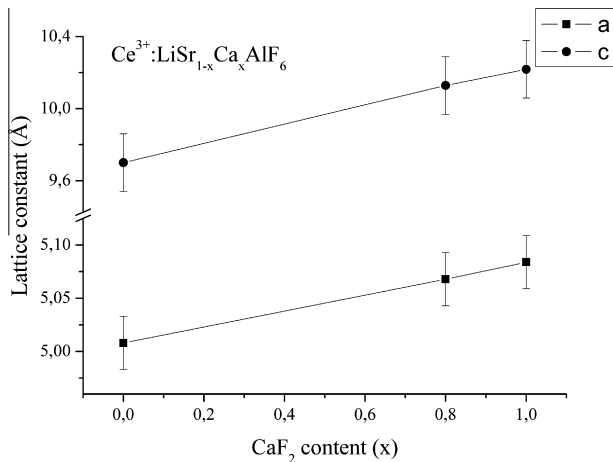**Fig. 1.** X-ray diffraction patterns of the samples of $Ce^{3+}:LiSr_{0.8}Ca_{0.2}F_6$ experimental data.

Fig. 2. Dependence of the lattice constants a and c of crystallized $Ce^{3+}:LiSr_{1-x}Ca_x$-AlF_6 material on the CaF_2 content.

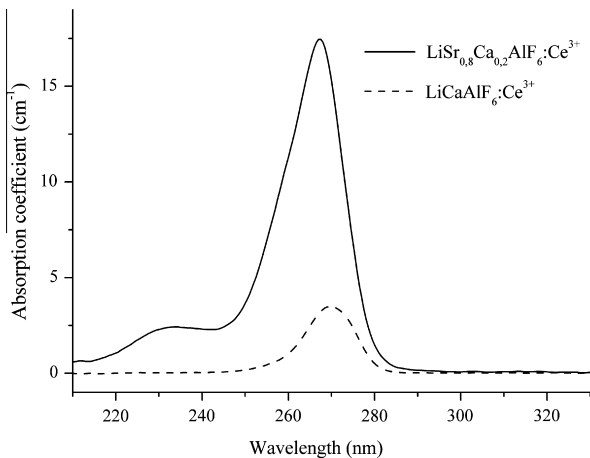**Fig. 3.** Unpolarized absorption spectra of $Ce^{3+}:LiCaAlF_6$ and $Ce^{3+}:LiSr_{0.8}Ca_{0.2}AlF_6$.

widely used to pump the Ce:LICAF active medium. Excitation at 266 nm provides both (a)- and (b)-impurity centers. Luminescence spectra at liquid nitrogen temperature were recorded to exclude the energy exchange between the different types of Ce^{3+} centers. Compared room and low temperature spectra, it is found that excitation at the shoulders of the absorption band excites a (b)-type center directly but an intense energy transfer to (c)-type center occurs in Ce:LICAF. The same process is taking place for an (a)-type center, which is excited directly at 266 nm but excitation is been transferred to (b)-type center. In a Ce:LICAF crystal, the relative intensity of a type (c)-center luminescence intensity is higher

than in a mixed LISCAF crystal. At the same time there is no any dramatic change in the luminescence time decay spectrum.

Typical luminescence time decays at 300 and 360 nm are associated to the interconfigurational 5d–4f transitions. The long wavelength side perturbed by excitons at liquid nitrogen is shown in Fig. 5. The time decays are owning to the overlapping of the luminescence bands of different Ce^{3+} centers, and the overlapping of the absorption bands leads to excitation of different types of Ce^{3+} ionic centers. For a 300 nm excitation, there is a smooth part of the decay curve indicating only a one component exponential time decay. However, the time resolution is limited from the pulse width of the excitation pulse of 10 ns. Here, the Ce^{3+} luminescence ionic decay is considered to be a single exponential one with a decay time of 29 ± 3 ns for both the LISCAF and LICAF matrices, in agreement with earlier observations [26]. This value is higher than [18], where the luminescence was affected by energy transfer between different types of Ce^{3+} centers at room temperature [19]. The decay time changes through the luminescence spectrum for both crystals and becomes relatively long (up to 50 ns) at the longer wavelengths (320–370 nm). Also, a nonexponential decay 200 ns after excitation was associated to a step-wise photoionization of Ce^{3+} ions and subsequent recombination [25,27,28].

In Fig. 6 the estimated luminescence decay times are presented with 10% deviation from the mean value. For excitation at 245 and 275 nm, (type (c)-center) there is an increment of the decay time due to reabsorption and energy exchange processes, which vanishes at liquid nitrogen temperature. There is not any differentiation between the Ce:LICAF and Ce:LISCAF lifetimes too. Therefore, any increment of absorption coefficient in mixed crystal is due to a concentration increment of the impurity centers, which was already observed for the mixed $LiF–LuF_3–YF_3$ crystals of scheelite structure [15].

So, for a mixed crystal type (c)-center, the relative concentration of Ce^{3+} ions is too low. It means that for a mixed LISCAF crystal, in contrast to Ce:LICAF one, only (a)- and (b)-types of Ce^{3+} ionic impurity centers are mainly formed. This behavior, where the excitation spectra coincide with the Ce^{3+} ionic absorption bands, Fig. 7, reflects a higher population inversion between the 5d- and 4f-states of Ce^{3+} ions, higher optical gain coefficients, broader tuning ranges and higher efficiency of laser action, following a crystal pumping with the 4-th harmonic of the Nd:YAG laser.

Overall, excitation spectra at different wavelengths do not show significant differences and their relative intensities are associated with the 4f–5d transitions of Ce^{3+} ions in Ce:LICAF and Ce:LISCAF crystals. This is obviously due to a significant energy exchange between different types of Ce^{3+} ionic centers at room temperature. Both LICAF and LISCAF crystals have a broad background excitation signature for the 350 nm fluorescence band, which corresponds to excitonic transitions [25]. Taking into account a significant enhancement of the 280–300 nm luminescence signal in the short wavelength shoulder of excitation spectrum and an intensity decrement of the (c)-type luminescence in Ce:LISCAF compared to Ce:LICAF, a concentration increment is taking place for only two impurity center types.
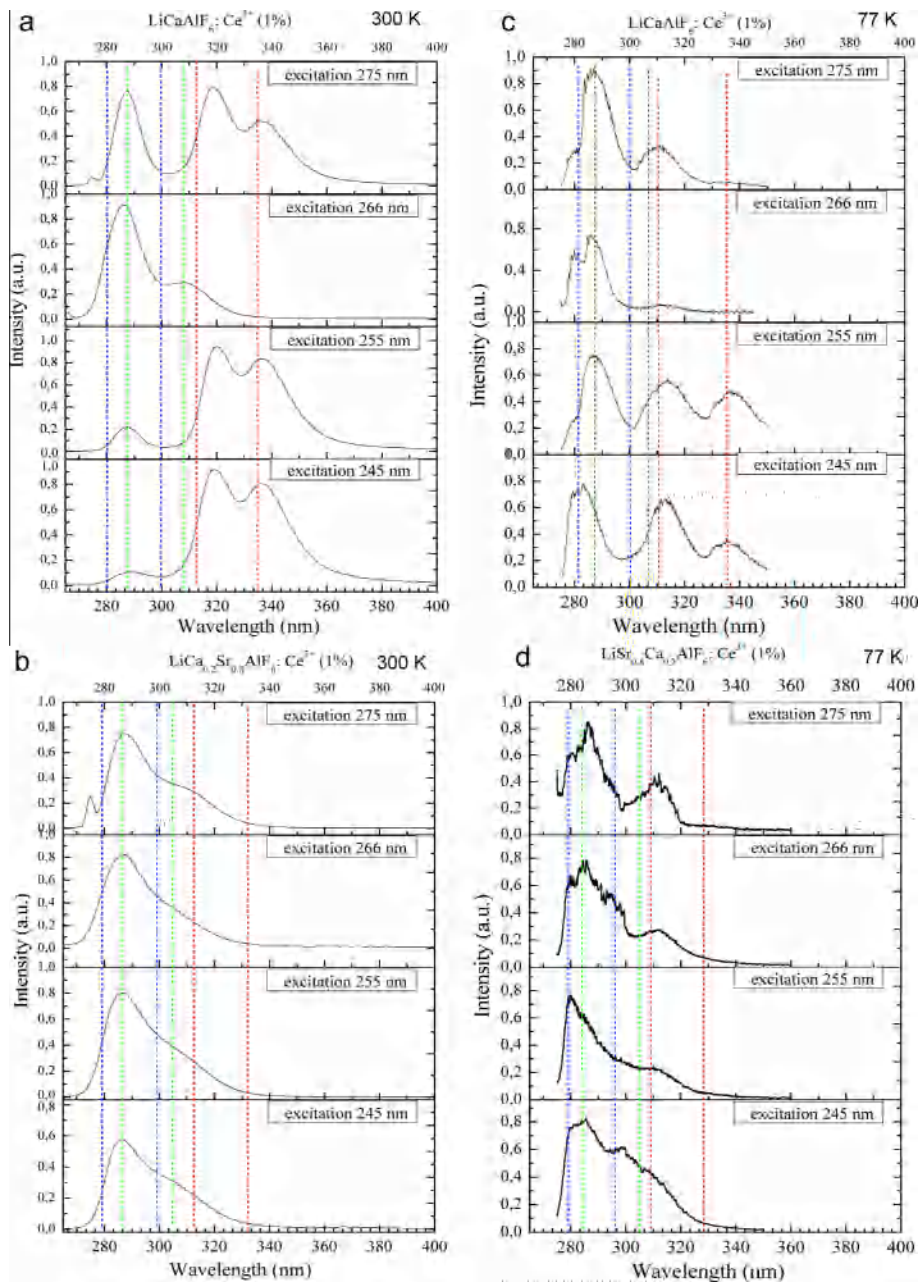
Fig. 4. Luminescence spectra of Ce³⁺:LiCaAlF₆ (a and c) and Ce³⁺:LiCa₀.₂Sr₀.₈F₆ (b and d) crystals at room temperature (a and b) and 77 K (c and d).
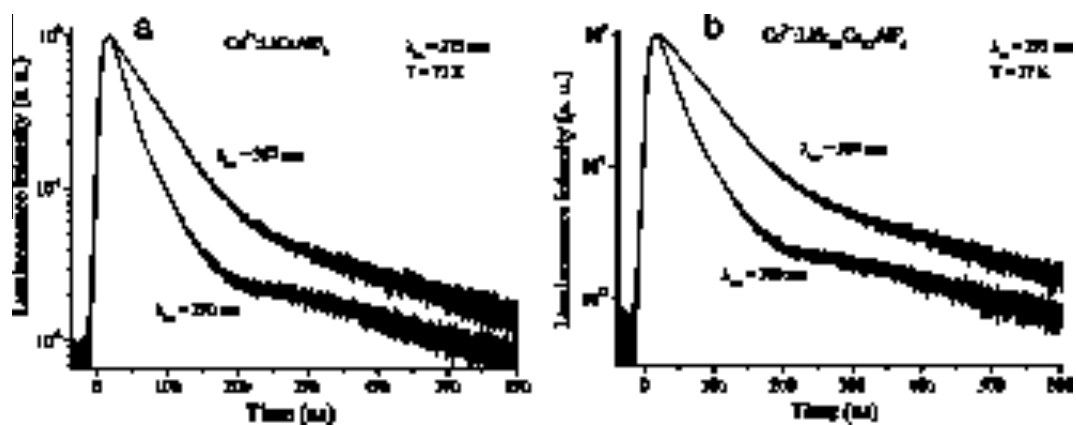
Fig. 5. Luminescence decay curves at 5d–4f transitions of Ce³⁺ ions in LiCaAlF₆ (a) and LiSr₀.₈Ca₀.₂AlF₆ (b) crystals under excitation at 275 nm at liquid nitrogen temperature.
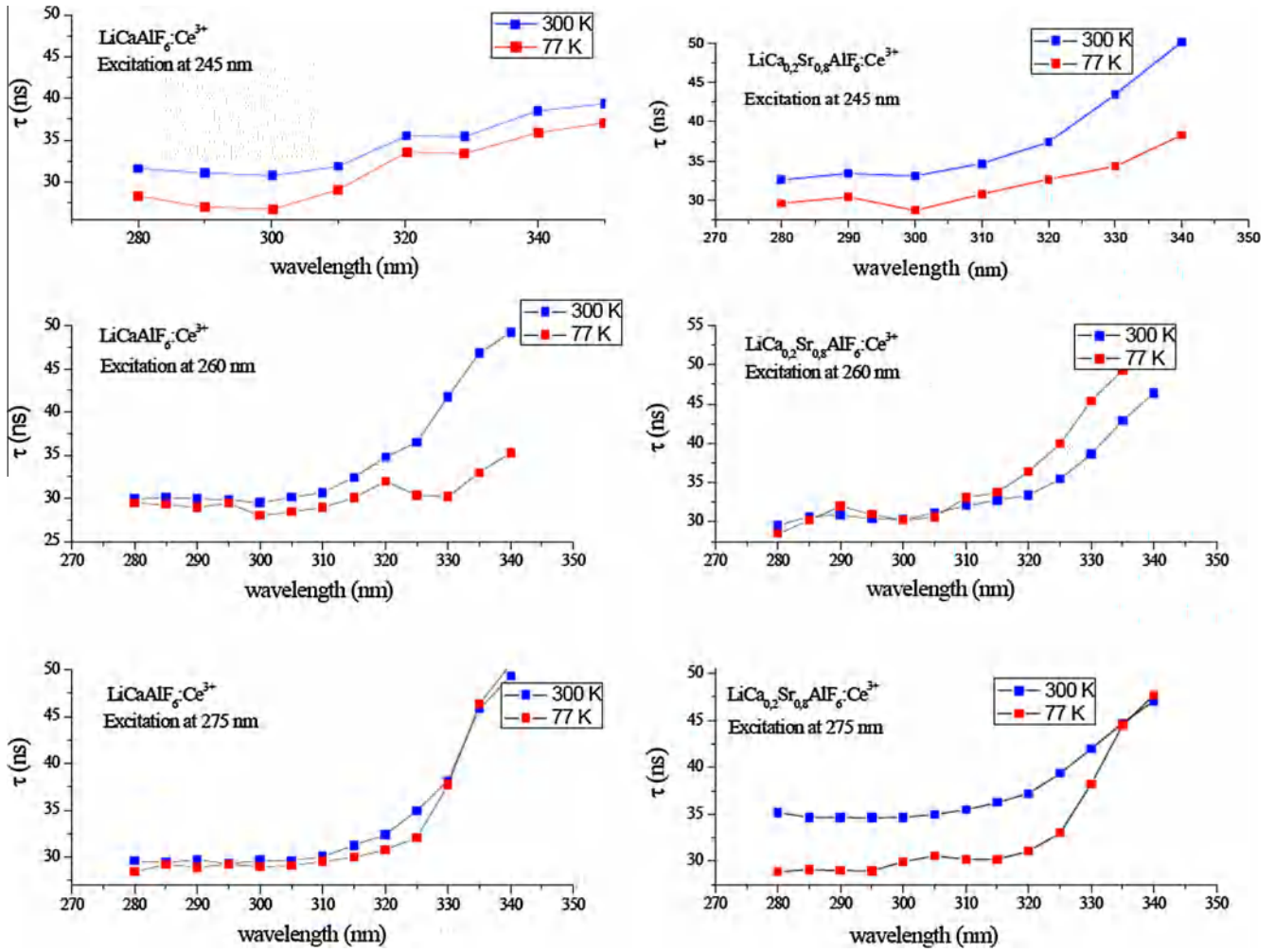
Fig. 6. Luminescence decay times τ spectral distribution of Ce^{3+} in $LiCaAlF_6$ (a, c and e) and $LiSr_{0.8}Ca_{0.2}F_6$ (b, d and f) host lattices at different registration wavelengths.

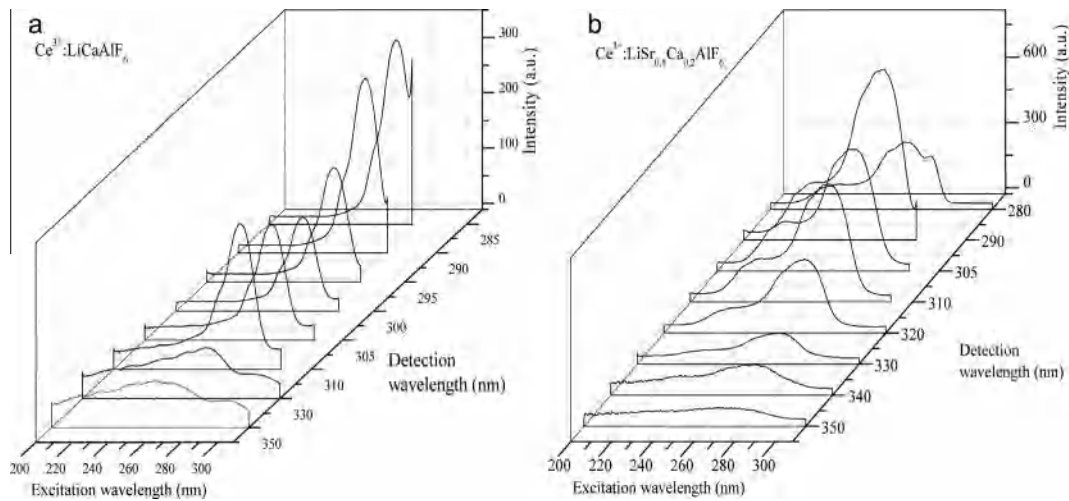**Fig. 7.** Excitation spectra of Ce^{3+}:$LiCaAlF_6$ (a) and Ce^{3+}:$LiSr_{0.8}Ca_{0.2}F_6$ (b) crystals at different registration wavelengths.

4. Conclusion

Mixed $LiSr_{0.8}Ca_{0.2}AlF_6$ crystals doped with Ce^{3+} ions were grown via the Bridgman–Stockbarger method. It is shown by X-ray diffraction that grown solid solutions of the $LiSr_{0.8}Ca_{0.2}AlF_6$ composition correspond to the colquiriite structure. There is a linear change of the lattice constant during the transition from the $LiCaAlF_6$ to the $LiSrAlF_6$ crystal and the crystals are single-phase. The absorption coefficient in mixed Ce:$LiSr_{0.8}Ca_{0.2}AlF_6$ crystals is higher than in Ce:$LiCaAlF_6$. Taking into account that there were

no significant differentiations of the 5d–4f lifetimes of the Ce^{3+} ionic centers, there is a higher segregation coefficient of the Ce^{3+} ions in mixed crystals. Only two Ce^{3+} ionic centers increase their concentration. By varying the chemical composition of the solid solution, the distribution and concentration of impurity centers can be controlled.

The results indicate a higher gain coefficient for the 5d–4f transitions of Ce^{3+} ions, a continuous tunability between 280 and 320 nm and a higher laser efficiency for the $Ce:LiSr_{0.8}Ca_{0.2}AlF_6$ crystal.

Acknowledgements

References

[1] M.A. Dubinskii, V.V. Semashko, A.K. Naumov, R.Y. Abdulsabirov, S.L. Korableva, Ce^{3+}-doped colquiriite. A new concept of all-solid-state tunable ultraviolet laser, J. Mod. Opt. 40 (1993) 1–5.

[2] Y. Yokota, Y. Fujimoto, et al., Growth and scintillation properties of Ce:Li(Ca, Ba)AlF$_6$ scintillator crystals, IEEE Trans. Nucl. Sci. 61 (2014) 419–423.

[3] B. Wellmann, D. Spence, D. Coutts, Tunable continuous-wave deep-ultraviolet laser based on Ce:LiCAF, Opt. Lett. 39 (2014) 1306–1309.

[4] L. Thanh, S. Schowalter, et al., Low-threshold ultraviolet solid-state laser based on a Ce^{3+}:LiCaAlF$_6$ crystal resonator, Opt. Lett. 37 (2012) 4961–4963.

[5] V.A. Fromzel, C.R. Prasad, K.B. Petrosyan, Y. Liaw, M.A. Yakshin, W. Shi, R. DeYoung, Tunable, narrow linewidth, high repetition frequency Ce:LiCAF lasers pumped by the fourth harmonic of a diode-pumped Nd:YLF laser for ozone DIAL measurements, in: Ki Young Kim (Ed.), Advances in Optical and Photonic Devices, INTECH, 2010, pp. 101–116.

[6] Z. Liu, K. Shimamura, K. Nakano, T. Fukuda, T. Kozeki, H. Ohtake, N. Sarukura, High-pulse-energy ultraviolet Ce^{3+}:LiCaAlF$_6$ laser oscillator with newly designed pumping schemes, Jpn. J. Appl. Phys., Part 2: Lett. 39 (2000) L466–L467.

[7] A.B. Petersen, C.D. Marshall, G.J. Quarles, High-repetition-rate Ce:LiCAF tunable UV laser, in: Conference Proceedings – Lasers and Electro-Optics Society Annual Meeting-LEOS, 1996, p. 110.

[8] D.J. Spence, H. Liu, D.W. Coutts, Low-threshold miniature Ce:LiCAF lasers, Opt. Commun. 262 (2006) 238–240.

[9] E. Granados, D. Coutts, D.J. Spence, Mode-locked deep ultraviolet Ce:LiCAF laser, Opt. Lett. 34 (2009) 1660–1662.

[10] V.V. Semashko, N. Sarukura, Z. Liu, A.K. Naumov, S.L. Korableva, Y. Segawa, R. Yu. Abdulsabirov, M.A. Dubinskii, Opt. Lett. 20 (1995) 599–601.

[11] M.H. Pham, M. Cadatal-Raduban, M.V. Luong, H.H. Le, K. Yamanoi, T. Nakazato, T. Shimizu, N. Sarukura, H.D. Nguyen, Numerical simulation of ultraviolet picosecond Ce:LiCAF laser emission by optimized resonator transients, Jpn. J. Appl. Phys. 53 (2014). 062701.

[12] L.H. Hai, N.D. Hung, A.V. Quema, G.A. Diwa, H. Murakami, S. Ono, N. Sarukura, Ce^{3+}-doped LiCaAlF$_6$ crystals as a solid-state ultraviolet saturable absorber and role of excited state absorption, Jpn. J. Appl. Phys. 44 (2005) 7984.

[13] D. Klimm, R. Uecker, P. Reiche, Melting behavior and growth of colquiriite laser crystals, Cryst. Res. Technol. 40 (2005) 352–358.

[14] N. Sarukura, Z. Liu, H. Ohtake, Y. Segawa, M.A. Dubinskii, V.V. Semashko, A.K. Naumov, S.L. Korableva, R.Yu. Abdulsabirov, Ultraviolet short pulses from an all-solid-state Ce:LiCAF master-oscillator power-amplifier system, Opt. Lett. 22 (1997) 994–996.

[15] A.S. Nizamutdinov, V.V. Semashko, A.K. Naumov, V.N. Efimov, S.L. Korableva, M.A. Marisov, On the distribution coefficient of Ce^{3+} ions in LiF–LuF$_3$–YF$_3$ solid-solution crystals, JETP Lett. 91 (2010) 23–25.

[16] V.K. Castillo, G.J. Quarles, R.S.F. Chang, Material and laser characterizations of intermediate compositions of $Ce:LiSr_xCa_{1-x}AlF_6$, J. Cryst. Growth 225 (2001) 445–448.

[17] V.K. Castillo, G.J. Quarles, R.S.F. Chang, Material and laser characterization of Ce, $Na:LiSr_xCa_{1-x}AlF_6$ compounds, Proc. SPIE 4970 (2003) 22–34.

[18] Z. Liu, T. Kozeki, Y. Suzuki, N. Sarukura, K. Shimamura, T. Fukuda, M. Hirano, H. Hosono, Ce^{3+}:LiCaAlF$_6$ crystal for high-gain or high-peak-power amplification of ultraviolet femtosecond pulses and new potential ultraviolet gain medium: Ce^{3+}:LiSr$_{0.8}$Ca$_{0.2}$AlF$_6$, IEEE J. Sel. Top. Quantum Electron. 7 (2001) 542–549.

[19] Semashko et al., Investigation of multisite activation in LiCaAlF$_6$:Ce^{3+} crystals using stimulated quenching of luminescence, Laser Phys. 5 (1995) 69–72.

[20] R.Yu. Abdulsabirov, M.A. Dubinskii, S.L. Korableva, A.K. Naumov, V.V. Semashko, V.G. Stepanov, M.S. Zhuchkov, Crystal growth, EPR and site-selective laser spectroscopy of Gd^{3+}-activated LiCaAlF$_6$ single crystals, J. Lumin. 94–95 (2001) 113–117.

[21] V.V. Semashko, Problems in searching for new solid-state UV- and VUV active media: the role of photodynamic processes, Phys. Solid State 47 (2005) 1507–1511.

[22] K. Shimamura, Growth of Ce-doped LiCaAlF$_6$ and LiSrAlF$_6$ single crystals by the Czochralski technique under CF$_4$ atmosphere, J. Cryst. Growth 211 (2000) 302.

[23] S. Kuze, D. du Boulay, et al., Structures of LiCaAlF$_6$ and LiSrAlF$_6$ at 120 and 300 K by synchrotron X-ray single-crystal diffraction, J. Solid State Chem. 177 (2004) 3505–3513.

[24] B. Rupp, W.L. Kway, J. Wong, P. Rogl, P. Fischer, Chromium site specific chemistry and crystal structure of LiCaCrF$_6$ and related chromium doped laser materials, J. Solid State Chem. 107 (1993) 471–479.

[25] T. Yanagida, A. Yoshikawa, Y. Yokota, S. Maeo, N. Kawaguchi, S. Ishizu, K. Fukuda, T. Suyama, Crystal growth, optical properties, and α-ray responses of Ce-doped LiCaAlF$_6$ for different Ce concentration, Opt. Mater. 32 (2009) 311–314.

[26] M.A. Dubinskii, V.V. Semashko, A.K. Naumov, R.Yu. Abdulsabirov, S.L. Korableva, Toward the understanding of the physically-limited operation of LiCAF:Ce tunable solid-state laser, OSA Proc. Adv. Solid-State Lasers 20 (1994) 222–226.

[27] A.S. Nizamutdinov, V.V. Semashko, A.K. Naumov, S.L. Korableva, R.Yu. Abdulsabirov, A.N. Polivin, M.A. Marisov, Optical and gain properties of series of crystals LiF–YF$_3$–LuF$_3$ doped with Ce^{3+} and Yb^{3+} ions, J. Lumin. 127 (2007) 71–75.

[28] V.V. Pavlov, Photodynamic processes in crystals LiCaAlF$_6$, LiY$_{1-x}$Lu$_x$F$_4$ and SrAlF$_5$ activated by Ce^{3+} ions, PhD thesis. <http://kpfu.ru/dis_card?p_id=1993>.